Research Article | Vol. 27, No. 4 | 18 Feb 2019 | OPTICS EXPRESS 5230
Optics EXPRESS

Simple analytical model for confinement loss estimation in hollow-core Tube Lattice Fibers

LUCA VINCETTI[1,*] AND LORENZO ROSA[1,2]

[1]*Department of Engineering "Enzo Ferrari", University of Modena and Reggio Emilia, via Vivarelli 10, I-41125 Modena, Italy*
[2]*Applied Plasmonics, Centre for Micro-Photonics, Swinburne University of Technology, P.O.Box 218, Hawthorn, VIC 3122, Australia*
[*]*luca.vincetti@unimore.it*

Abstract: In this work, we propose an analytical model for estimating confinement loss in Tube Lattice Fibers. It is based on the single-tube model and the inhibited coupling waveguiding mechanism. The comparison with numerical simulations of tube lattice fibers having different geometrical parameters and dielectric refractive indexes demonstrates the model validity and effectiveness. Being based only on analytical closed formulas, it constitutes a useful tool for rapid estimation of TLF CL. It also gives a more in-depth insight into the TLF guiding mechanisms, confirming the inhibited coupling is an appropriate and effective model for such kind of fibers.

1. Introduction

Since they were first proposed [1], and then experimentally demonstrated [2], single-ring Tube Lattice Fibers (TLFs) have been showing extremely interesting optical properties, making them good candidates as hollow-core low-loss broadband fibers for applications from the terahertz band [3, 4] to visible and ultraviolet wavelengths [5, 6], including the mid-infrared [7, 8] spectral range. More recently they have proved to be also a good platform for sensing [9–11].

Their waveguiding mechanism is known as Inhibited Coupling (IC): it is the same as Kagome Fibers and is based on the inhibition of the coupling between core modes and cladding ones [12, 13]. The waveguiding of these fibers is also referred to in the context of ARROW. We refer the reader to [5, 14], which explain the differences. A consequence of the guidance mechanism is the leaky nature of the core modes, so that Confinement Loss (CL) is one of the main loss mechanisms in TLFs. Recently, an empirical formula able to estimate the minimum value of CL in each of the fiber transmission bands has been proposed [15].

In this work we further extend the model, taking into account the high-loss bands separating the fiber transmission bands. Preliminary results have been shown in [16]. Here we report a more in depth description of the model and of the analytical formulas used, and we extend the validation to a wider range of fibers. The approach here followed is based on the single-tube model [1, 3]. That model describes the cladding modes in terms of the modes of a single dielectric tube, which have been analytically calculated in closed form [17]. In particular, the high-loss spectral bands are defined by the cut-off frequencies of the cladding modes, which are well approximated by the cut-off frequencies of the single-tube modes [1]. By assuming that the loss caused by the coupling between a core mode and a single cladding mode manifests itself as a function with a Lorentzian spectral shape, it is possible to estimate the loss in the high-loss band. Combining this formalism with the formula estimating the CL minima in each transmission band, it is possible to obtain an accurate analytical model for TLF CL.

The model is validated by comparing its analytical results with numerical simulations of several TLFs with different geometrical parameters and refractive indexes working in different spectral ranges. In all cases, the good agreement shows the validity and the effectiveness of the model. The proposed analytical model not only permits to obtain a quicker estimate of the loss, but also to gain more insight in the waveguiding process.

#348810 https://doi.org/10.1364/OE.27.005230
Journal © 2019 Received 29 Oct 2018; revised 16 Dec 2018; accepted 18 Dec 2018; published 12 Feb 2019

Optics EXPRESS

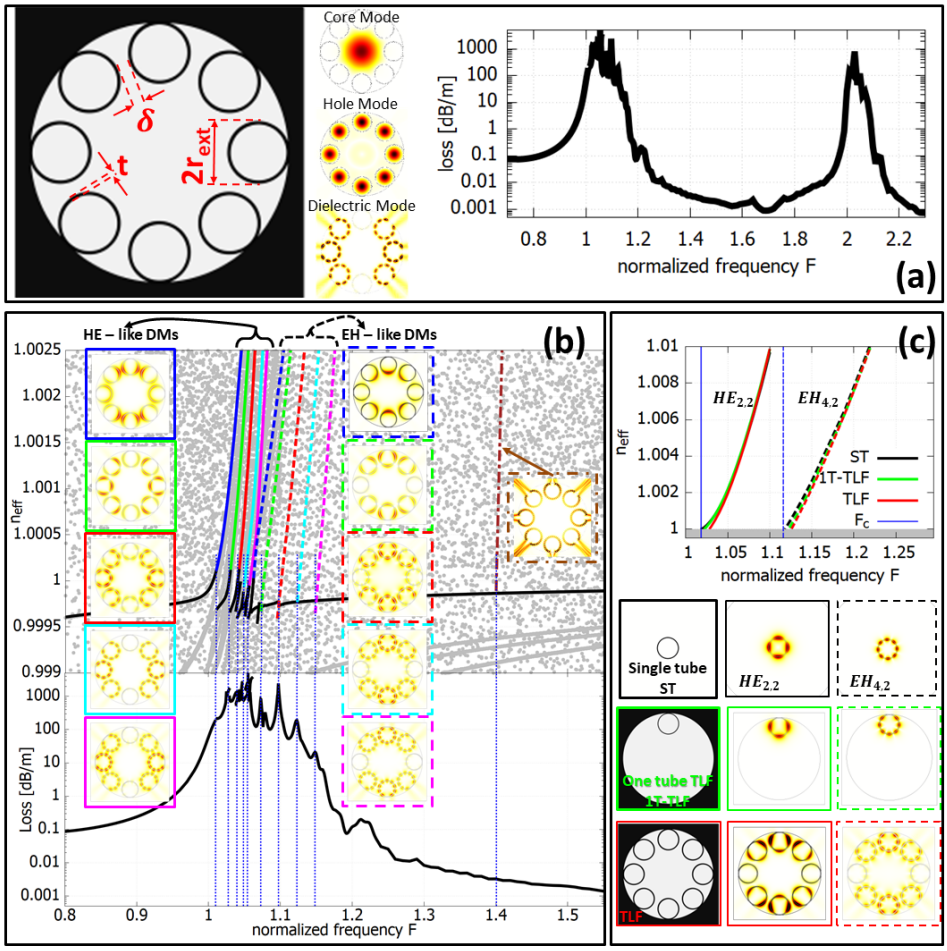

Fig. 1. (a) Left: Geometry of TLF cross-section; center: E-field magnitude distribution examples of core, hole, and dielectric modes; right: CL spectrum. (b) TLF mode dispersion map (top) and fundamental mode confinement loss (bottom) around $F = 1$; in the dispersion map, the gray dots represent the effective indexes of cladding modes; the dispersion curves of DMs with slow spatial oscillation are shown with colored solid and dashed lines, for HE-like and EH-like modes, respectively; the corresponding electric field distributions are shown in the insets; the brown dashed-dotted line shows the dispersion curve of a quickly spatially oscillating DM; the dotted blue lines shows the FM-DMs phase-matching frequencies, corresponding to peaks in the loss spectrum (except for the DM with quick oscillations). (c) Single-tube model validation. Top: Dispersion curves of HE (solid) and EH (dashed) modes with same oscillation period along the tube perimeter and the same profile across the tube boundary orthogonal direction. Bottom: Cross-sections of the analyzed fibers and electric field distributions of the two kinds of modes compared in the analysis.

2. Model description

Differently from Photonic Band Gap Fibers, the cladding of Inhibited Coupling Fibers (ICFs) does not exhibit any kind of band gap and the cladding modes (CLMs) form a continuum of highly lossy solutions [12]. A core mode (CM) is potentially coupled with lossy CLMs at any wavelength, since there is always a CLM having the same effective index (fulfilling the phase matching condition) as the CM. Despite that, CM loss spectra are composed of an alternation

Optics EXPRESS

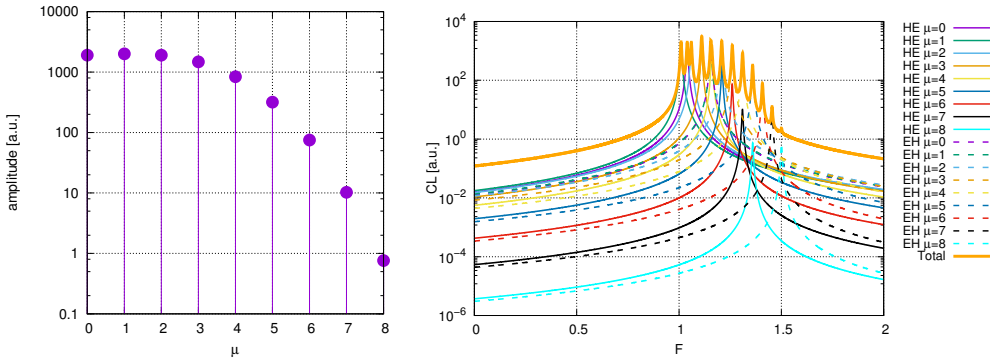

Fig. 2. Left: Amplitudes of the Lorentzian resonances of the CLMs. Right: $p_\nu(F)$ (thick solid line), $L(F - F^{HE}_{c_{\mu,\nu}})$ (solid lines), and $L(F - F^{EH}_{c_{\mu,\nu}})$ (dashed lines) spectra for $\nu = 2$, $\mu \leq 8$, $r_{ext} = 5\mu m$, $t = 1\mu m$, and $n = 1.44$.

of high- and low-loss bands. High-loss bands correspond to phase matching between CMs and CLMs with slow spatial oscillations on the fiber transverse plane [5, 12]. Low-loss ones correspond to spectral bands where only CLMs with quick oscillations are present. Since in a hollow-core fiber, the effective index of CMs is lower than but close to the air line, the phase matching condition occurs very close to the cut-off of the latter. CM loss spectra are thus mainly defined by the spectral distribution of the CLM cut-off wavelengths.

TLFs are a particular kind of ICFs where the microstructured cladding is composed only of a ring of dielectric tubes surrounding the hollow core, and surrounded in turn by a homogeneous dielectric. Here t, r_{ext}, δ, and N are thickness, external radius, spacing, and number of the tubes composing the cladding. An example of TLF with $N = 8$ is shown in Fig. 1(a) together with an example of the three kind of modes sustained by TLFs: cladding dielectric modes (DMs) mainly confined within the tubes' dielectric, core modes (CMs) confined in the hollow core, and hole modes (HMs) mainly confined inside the tubes' holes. Since usually the core radius R_{co} is larger than $r_{ext} - t$ and we will focus on the CL of the fundamental core mode (FM), HMs do not play any role and for this reason they will not be examined here. The reader can find a thorough analysis about their role in TLF waveguiding in the following references [1, 15, 18]. Figure 1(a) also shows a typical FM CL spectrum. F is the normalized frequency: $F = 2t/\lambda\sqrt{n^2 - 1}$, being λ the wavelength and n the refractive index of the dielectric. The TLF has a number of tubes $N = 8$ and parameters: $t = 0.6\mu m$, $r_{ext} = 9\,\mu m$, $\delta = 4.2\mu m$, and $n = 1.45$. The spectrum is an alternation of low loss regions and high loss ones occurring at the vicinity of integer values of F. Figure 1(b) shows a detail of the mode dispersion map centered around the high-loss peak at $F = 1$. Gray dots correspond to the effective indexes of the DMs. The FM dispersion curve is highlighted in black. Also, the dispersion curves of DMs with slow spatial oscillation are highlighted with different colors and style lines, according to the number of spatial periods along the tubes' perimeter and polarization (electric field tangential - HE-like - or orthogonal - EH-like - to tubes' boundaries). The anti-crossings due to the coupling between FM and DMs with slow spatial oscillation are clearly visible. In the same figure also the CL spectrum of the FM is shown. It highlights that the high-loss band is actually composed of several peaks with the maxima centered at the frequencies corresponding to the phase matching between FM and DMs. Also, the strength of the anti-crossing and the peak amplitude is reduced as the DM spatial field oscillations become quicker and quicker. A field distribution of a mode with quick spatial oscillations is also shown (coded in brown). Its dispersion curve intersects the FM one with no observable anti-crossing at the plot resolution used here, and also no peak is observed in the CL spectrum. This is explained by coupled mode theory, which states that the coupling between two

Optics EXPRESS

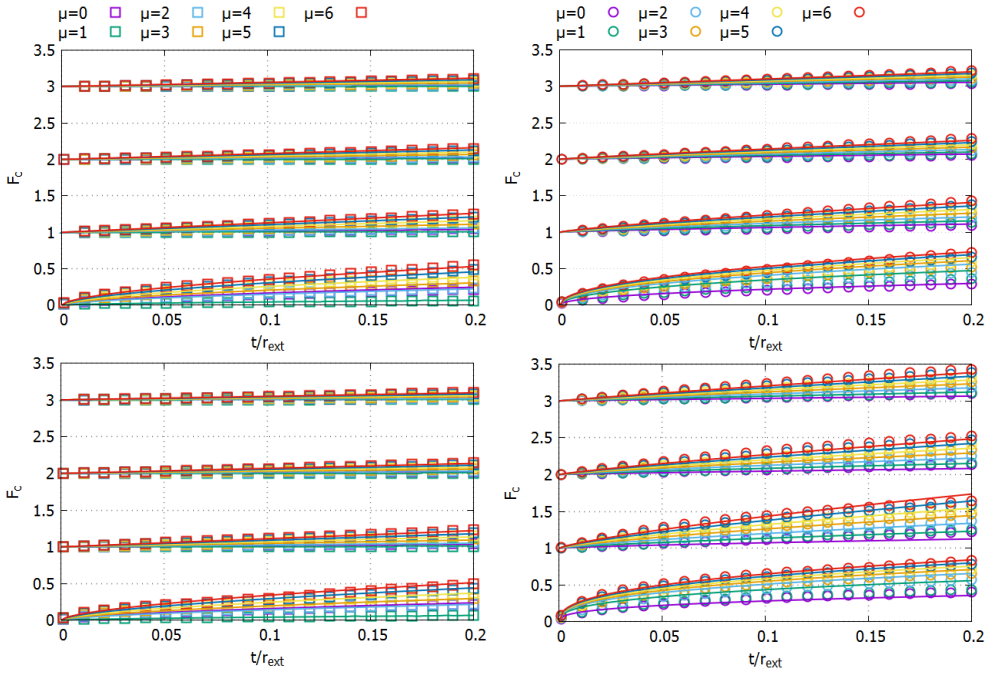

Fig. 3. Cut-off normalized frequencies of the dielectric tube modes $HE_{\mu,\nu}$ (left) and $EH_{\mu,\nu}$ (right) as a function of tube aspect-ratio parameter t/r_{ext} for two different refractive indexes: $n = 1.44$ (top), and $n = 2.5$ (bottom). Symbols refer to numerical solutions, solid lines to approximated analytical formulas.

modes occurs when the phase matching condition is satisfied and it is stronger as the overlap integral

$$k = \frac{\pi}{2\lambda} \int_{S_\infty} \vec{E}_{FM} \cdot \vec{E}_{DM} dS \tag{1}$$

is greater than zero [5].

Since the high-loss peaks are a superposition of peaks corresponding to the coupling of the core mode with a slow spatial oscillation DM, their peak bandwidth depends on the spectral distribution of the cut-off frequencies of the slow spatial oscillation DMs. According to the single-tube model [1], these cut-off frequencies can be estimated with those of the dielectric modes of a single-tube (ST) fiber. The fairness of the single-tube approximation can be appreciated in Fig. 1(c), where the dispersion curve and electric field distribution of two TLF DMs are compared with those of a ST fiber and with those of a TLF having only one tube in the cladding (1T-TLF). The compared modes have same spatial period along the tube's perimeter and same profile across the tube's thickness. The dispersion curves are almost overlapping and the cut-off frequency difference is of the order of 1%.

The advantage of the single-tube model relies on the fact that the modes of a ST fiber have been analytically analyzed in [17]. Their cut-off can be effectively expressed in terms of two normalized quantities: the normalized frequency F and the tube aspect-ratio t/r_{ext}. They also depend on the refractive index of the dielectric. The higher the refractive index the more spread out the cut-off frequencies. Figure 3 shows the cut-off normalized frequencies F_c obtained numerically solving the transcendental dispersion equations for two different refractive indexes. The indexes μ and ν, represent the azimuthal and radial index, respectively.

Optics EXPRESS

In the proposed approach, each FM-DM resonance is modeled with a Lorentzian-shaped peak:

$$L(F) = \frac{\gamma^2}{\gamma^2 + F^2}, \tag{2}$$

with $\gamma = 0.003$. Each peak is centered at one of the ST fiber cut-off frequencies $F_{c_{\mu,\nu}}^{HE}$, $F_{c_{\mu,\nu}}^{EH}$. Their peak amplitudes $A(\mu)$ have to take into account that the coupling strength is reduced as the azimuthal index μ is increased [5]. Here we propose the following empirical formula:

$$A(\mu) = 2 \cdot 10^3 e^{-0.05|\mu-1|^{2.6}}. \tag{3}$$

Plots of the amplitudes for $\mu \leq 8$ are shown in Fig. 2. The origin of the value of γ in Eq. (2) and the expression of Eq. (3) is purely empirical, however their validity is verified by the result analysis shown and discussed in the next section.

Even though analytical solutions of the ST fiber modes are available [17], their cut-off normalized frequencies F_c are only available as solutions of transcendental equations. To further simplify the model and avoid numerical integrations, here we also propose approximated analytical formulas for the estimation of F_c:

$$F_{c_{\mu,\nu}}^{HE} = \begin{cases} \left|0.21 + 0.175\mu - \dfrac{0.1}{(\mu - 0.35)^2}\right| \left(\dfrac{t}{r_{ext}}\right)^{\left(0.55+5\cdot 10^{-3}\sqrt{n^4-1}\right)} + 0.04\sqrt{\mu}\left(\dfrac{t}{r_{ext}}\right) & \text{if } \nu = 1 \\ \dfrac{0.3}{n^{0.3}}\left(\dfrac{2}{\nu}\right)^{1.2} |\mu - 0.8| \left(\dfrac{t}{r_{ext}}\right) + \nu - 1 & \text{if } \nu \geq 2 \end{cases} \tag{4}$$

$$F_{c_{\mu,\nu}}^{EH} = \begin{cases} \left(0.73 + 0.57\dfrac{\mu^{0.8} + 1.5}{4} - \dfrac{0.04}{\mu - 0.35}\right) \left(\dfrac{t}{r_{ext}}\right)^{0.5 - \frac{n-1}{10(\mu+0.5)^{0.1}}} & \text{if } \nu = 1 \\ \dfrac{11.5}{\nu^{1.2}(7.75 - \nu)} \dfrac{0.34 + \dfrac{\mu}{4}\left(\dfrac{n}{1.2}\right)^{1.15}}{(\mu + \frac{0.2}{n})^{0.15}} \left(\dfrac{t}{r_{ext}}\right)^{\left(0.75 + \frac{0.06}{n^{1.15}} + 0.1\sqrt{\frac{1.44}{n}}(\nu-2)\right)} + \nu - 1 & \text{if } \nu \geq 2 \end{cases} \tag{5}$$

Again, despite the empirical origin of these expressions, their validity has been verified by comparing the exact numerical solutions of transcendental equations and the approximated analytical ones as shown in Fig. 3. There is a good agreement in the range of t/r_{ext} of practical interest.

Finally, in the proposed model, the FM confinement loss of TLFs is estimated as:

$$CL_{an}(F) = \sum_{\nu} p_\nu(F) \cdot CL_{min}(F), \tag{6}$$

with

$$p_\nu(F) = \sum_{\mu} A(\mu) \left(L(F - F_{c_{\mu,\nu}}^{HE}) + L(F - F_{c_{\mu,\nu}}^{EH})\right), \tag{7}$$

and $CL_{min}(F)$ is the function giving the minimum value of CL_{an} in each transmission band [15]. Here, in Eq. (3) of [15], the minimum value $3 \cdot 10^{-4}$ instead of the average value $5 \cdot 10^{-4}$ has been used. Examples of $p_\nu(F)$, $L(F - F_{c_{\mu,\nu}}^{HE})$, $L(F - F_{c_{\mu,\nu}}^{EH})$ spectra for $\nu = 2$ and $\mu \leq 8$ are shown in Fig. 2.

Optics EXPRESS

Table 1. TLF design parameters for different spectral ranges.

Fiber	t (μm)	r_{ext} (μm)	δ (μm)	n	N	Spectral range
F#1	1.0	10	5.0	1.44	8	NIR
F#2	1.0	5.0	2.5	1.44	8	NIR
F#3	1.0	10	2.5	1.44	8	NIR
F#4	0.5	10	5.0	1.44	8	VIS
F#5	0.2	4.0	0.419	1.50	8	UV
F#6	0.2	4.0	1.6	1.50	8	UV
F#7	1.0	10	5.0	1.44	6	NIR
F#8	1.0	10	5.0	2.42	8	MIR
F#9	1.0	10	4.0	1.44	10	NIR
F#10	100	1000	445	1.521	8	THz

To summarize, according to the inhibited coupling waveguiding mechanism, the high-loss bands p_ν are the results of the superposition of the loss coming from the resonance of the FM with DMs having slow transverse spatial oscillation. In the proposed model, we describe the single resonance loss curve with a Lorentzian function $L(F)$, estimating the spectral location by means of the cut-off frequencies of the ST fiber modes $F^{HE}_{c_{\mu,\nu}}$ and $F^{EH}_{c_{\mu,\nu}}$. CL_{an} is estimated combining the high-loss term p_ν with the function giving the minimum value in each transmission band CL_{min}.

3. Model validation

In order to validate the model, and in particular the validity of the empirical formulas proposed to estimate bandwidth and amplitude of the single Lorentz resonance, ten different TLF designs have been considered. The fibers covers different spectral ranges: ultraviolet (UV), visible and near infrared (NIR), mid infrared (MIR), and THz. The design parameters are summarized in Table 1. The geometrical parameters range over about 3 orders of magnitude, and the dielectric refractive index from 1.44, that is the refractive index of the silica in NIR, to 2.42, that is the refractive index of chalcogenide glass such as As_2S_3 in MIR. A number of tubes between 6 and 10 has been considered because it is the range usually used in real fibers. Fibers with significantly different tube aspect ratios have been compared, as that ratio significantly affects the DM cut-off normalized frequencies and thus the spectral width of the high-loss bands [1]. The same is for the dielectric refractive index. Also, fibers with significantly different core radius have been considered in order to check if the loss peaks p_ν could affect the effectiveness of the CL_{min} analytical formula for the minimum loss estimation inside each transmission band. The validation has been carried out by comparing the CL estimation with the analytical model here proposed with numerical CL spectra obtained with COMSOL Multiphysics. The comparisons of the ten fibers (from #1 to #10) are shown in Fig. 4. The analysis covers the first four transmission bands. To better appreciate the accuracy also the ratio CL_{an}/CL_{num} is shown. In the CL_{an} computation only the cladding modes with $\mu \leq 8$ have been considered. Analytical formulas agree quite well with the numerical results over a wide spectral range covering the first four transmission bands. By focusing on the low-loss spectral bands, where the fibers are actually used, the agreement is

Optics EXPRESS

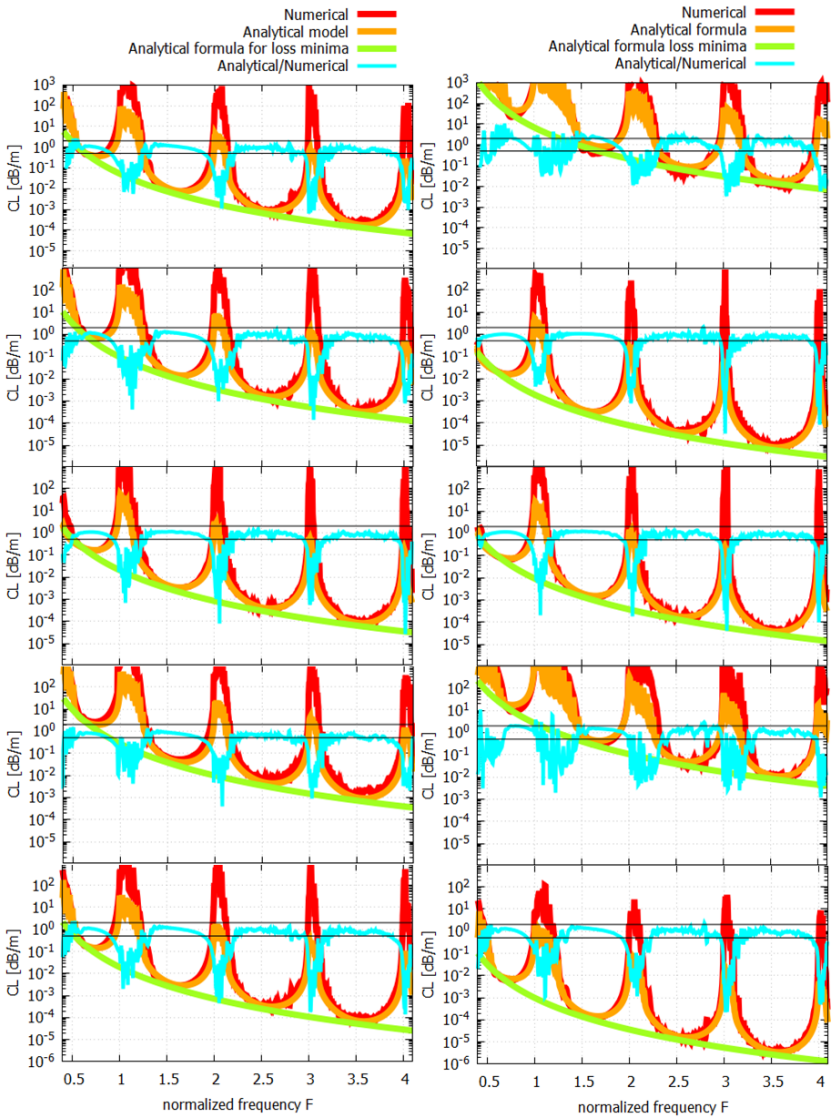

Fig. 4. CL spectra for Fibers from #1 to #10 (left-right, top-down) given by numerical simulations (red curve) and analytical model (orange curve), and their ratio (cyan curve). The curve from the analytical formula for the minima proposed in [15] is also shown in green colour. The solid black lines represent values of 2.0 and 0.5 for the ratio.

good for all fibers even though CL ranges from more than $10dB/m$ to less than $10^{-5}dB/m$ for a total of about seven order of magnitude. The ratio CL_{an}/CL_{num} is bound between 0.5 and 2 over wide range in each transmission band. The worst agreement is in Fiber #2, which is the fiber with the highest aspect ratio $t/r_{ext} = 0.2$. However, such high aspect ratios are hardly ever used in practice, due to the narrow band of the low loss regions and due to CL scaling as $(t/r_{ext})^6$ [15].

4. Conclusion

In this work we proposed an analytical model to estimate CL inside TLF transmission bands. It is based on the Inhibited Coupling guiding mechanism to model the interaction between core

Optics EXPRESS

modes and cladding modes, and on the single-tube model for the description of the cladding modes in TLFs. Resonances between fundamental core mode and cladding modes are spectrally estimated by considering the single-tube dielectric modes, and modeled as Lorentzian resonances. The high-loss peaks so obtained are combined with an empirical formula for the minimum loss estimation previously proposed by one of the authors. Albeit the analytical formulas for estimation of frequencies and amplitudes of the resonances could appear a little exotic, their effectiveness has been demonstrated through the analysis of ten TLFs with different geometrical parameters and refractive indexes, covering all spectral range of TLF applications from THz to UV. A good agreement between the proposed model confinement loss estimation and its numerical computation is observed inside the first four transmission bands even though the geometrical parameters have been varied over two orders of magnitude and the loss range over seven orders of magnitude. The model is completely based on analytical closed formulas which can also be easily implemented in a spreadsheet, constituting a useful tool for rapid estimation of TLF CL. It also helps to give a more in-depth insight into the TLF guiding mechanisms, confirming the inhibited coupling is an appropriate and effective model to describe and analyze waveguiding in this kind of fibers.

References

1. L. Vincetti and V. Setti, "Waveguiding mechanism in tube lattice fibers," Opt. Express **18**, 23133–23146 (2010).
2. A. D. Pryamikov, A. S. Biriukov, A. F. Kosolapov, V. G. Plotnichenko, S. L. Semjonov, and E. M. Dianov, "Demonstration of a waveguide regime for a silica hollow - core microstructured optical fiber with a negative curvature of the core boundary in the spectral region $> 3.5\ \mu$m," Opt. Express **19**, 1441–1448 (2011).
3. V. Setti, L. Vincetti, and A. Argyros, "Flexible tube lattice fibers for terahertz applications," Opt. Express **21**, 3388–3399 (2013).
4. H. Li, G. Ren, B. Zhu, Y. Gao, B. Yin, J. Wang, and S. Jian, "Guiding terahertz orbital angular momentum beams in multimode Kagome hollow-core fibers," Opt. Lett. **42**, 179–182 (2017).
5. B. Debord, A. Amsanpally, M. Chafer, A. Baz, M. Maurel, J. M. Blondy, E. Hugonnot, F. Scol, L. Vincetti, F. Gérôme, and F. Benabid, "Ultralow transmission loss in inhibited-coupling guiding hollow fibers," Optica **4**, 209–217 (2017).
6. M. Cassataro, D. Novoa, M. C. Günendi, N. N. Edavalath, M. H. Frosz, J. C. Travers, and P. S. Russell, "Generation of broadband mid-ir and uv light in gas-filled single-ring hollow-core pcf," Opt. Express **25**, 7637–7644 (2017).
7. A. N. Kolyadin, A. F. Kosolapov, A. D. Pryamikov, A. S. Biriukov, V. G. Plotnichenko, and E. M. Dianov, "Light transmission in negative curvature hollow core fiber in extremely high material loss region," Opt. Express **21**, 9514–9519 (2013).
8. R. R. Gattass, D. Rhonehouse, D. Gibson, C. C. McClain, R. Thapa, V. Q. Nguyen, S. S. Bayya, R. J. Weiblen, C. R. Menyuk, L. B. Shaw, and J. S. Sanghera, "Infrared glass-based negative-curvature anti-resonant fibers fabricated through extrusion," Opt. Express **24**, 25697–25703 (2016).
9. C. Wei, J. T. Young, C. R. Menyuk, and J. Hu, "Temperature sensor using fluid-filled negative curvature fibers," in "Conference on Lasers and Electro-Optics," (Optical Society of America, 2018), p. JW2A.179.
10. X. lu Liu, W. Ding, Y. ying Wang, S. fei Gao, L. Cao, X. Feng, and P. Wang, "Characterization of a liquid-filled nodeless anti-resonant fiber for biochemical sensing," Opt. Lett. **42**, 863–866 (2017).
11. F. Giovanardi, A. Cucinotta, and L. Vincetti, "Inhibited coupling guiding hollow fibers for label-free dna detection," Opt. Express **25**, 26215–26220 (2017).
12. F. Couny, F. Benabid, P. J. Roberts, P. S. Light, and M. G. Raymer, "Generation and photonic guidance of multi-octave optical-frequency combs," Science **318**, 1118–1121 (2007).
13. A. Argyros and J. Pla, "Hollow-core polymer fibres with a kagome lattice: potential for transmission in the infrared," Opt. Express **15**, 7713–7719 (2007).
14. F. Yu and J. C. Knight, "Negative curvature hollow-core optical fiber," IEEE Journal of Selected Topics in Quantum Electronics **22**, 146–155 (2016).
15. L. Vincetti, "Empirical formulas for calculating loss in hollow core tube lattice fibers," Opt. Express **24**, 10313–10325 (2016).
16. L. Rosa and L. Vincetti, "Analytical estimation of confinement loss in tube lattice fibers," in "Advanced Photonics 2018," (Optical Society of America, 2018), p. JTu5A.65.
17. M. M. Z. Kharadly and J. E. Lewis, "Properties of dielectric-tube waveguides," Proc. IEE **116**, 214–224 (1969).
18. P. Uebel, M. C. Günendi, M. H. Frosz, G. Ahmed, N. N. Edavalath, J.-M. Ménard, and P. S. Russell, "Broadband robustly single-mode hollow-core pcf by resonant filtering of higher-order modes," Opt. Lett. **41**, 1961–1964 (2016).